Clinical Applications Of Computer Models For Strabismus

Joel M Miller, PhD [1], and Joseph L Demer, MD, PhD [2]

[1] Smith-Kettlewell Eye Research Institure, San Francisco

[2] Jules Stein Eye Institute, UCLA

Introduction

Diagnosis and treatment of strabismus are based mostly on simple heuristics, shared experience and intuition. Consequently, unusual and complex strabismus cases may be difficult to manage. A description of the mechanisms of binocular coordination – a model – attacks these problems in a new way: experience, intuition and experimental findings go into building and testing the model, and then the model, less impaired by unfamiliarity and complexity, is used in case management.

A model-driven approach, able to coordinate broad ranges of laboratory research and clinical experience, can accelerate progress in diagnosis and treatment of strabismus. Without analytical methods it is difficult to develop useful new procedures, particularly for complex, cyclovertical disorders. Indeed, such developments have been infrequent. As prosthetic extraocular muscles (EOMs) become practical (Bicas, 1972; Scott, et al, 1992) their use will require judgments for which computational analysis provides the most appropriate guidance.

Actions of the oblique EOMs are complex (Neetens and Janssens, 1979; Miller and Robinson, 1984), and dysfunction is often not obvious from inspection of ocular ductions and versions (Burgerman, et al, 1989). It is possible that most strabismus is complex, involving abnormal contractile and elastic forces, and path changes in several muscles, their innervations, and their connective tissue suspensions. In many cases of congenital and traumatic strabismus, the primary lesions are obviously multiple and complex. But even in an isolated palsy, there will generally be secondary changes in other muscles: it is well known that muscles adapt to changes in their working length (Williams and Goldspink, 1978; Scott, 1994). Innervational changes due to plasticity of neural control centers are less well understood, but are probably important in many disorders. It may be that strabismus diagnoses are typically simple (and so, it would follow, incomplete) because they are based on limited, poorly-controlled alignment measurements (Demer, et al, 1992). Such measurements may be the norm because it is impossible to assimilate more adequate data without computational help.

Orientation to Strabismus Models

What types of analytical models are available to help with strabismus diagnosis and treatment?

Empirical generalizations

A type of model familiar to strabismus surgeons is the ***empirical generalization***, examples of which are the familiar tabular surgical "dose-response" relationships (eg, (Parks and Wheeler, 1996)), and the computer programs of Russman (Rüssman, 1982), Konen and Russman (Konen and Rüssman, 1982), and Simonsz (Simonsz, 1990). Whether developed informally, or with computerized databases and statistical techniques, empirical generalizations summarize experience; they are *models of observations*. Empirical generalizations are probably the basis of professional competence in most fields. However, because they are so closely related to experience, empirical generalizations may seem

correct, even if flawed. Thus, they may impede fundamental progress by instilling a sense of understanding without explaining the causes of observed patterns. Nevertheless, empirical generalizations have been, and will continue to be of great value in strabismus management.

Expert systems

An ***expert system*** is a different kind of model, not of the topics of interest themselves (gaze angles, muscles, etc.), but of the inferences and judgments of human experts. Expert systems are *psychological models*. Their strength is derived from their extreme domain-specificity (Hayes-Roth, et al, 1983), which at the same time limits their generality. Expert systems are perhaps best thought of as ways to distribute extant professional expertise, rather than as means to fundamentally advance a field. Expert systems may also find roles in strabismus education and practice.

Homeomorphic models

Neither empirical generalizations nor expert systems can put strabismology on a scientific basis, since neither treats the subject matter in terms of mechanisms: lawful relationships among subprocesses or parts of the oculomotor system. Non-mechanistic models have difficulty with new situations, since there may be no way to know if their similarity to known situations is merely superficial, and they tend not to have implications outside the problem area for which they were developed.

A ***homeomorphic model*** is a mechanistic model that has the "same form" as the system modeled: the model has parts that correspond to physiologic structures, and the interactions of model parts reflect physiologic processes. A homeomorphic model can treat arbitrary new situations, so long as they can be expressed using the model's terms. Successful predictions validate the model. Unsuccessful predictions tend to specify the physiologic research needed to improve the model.

Biomechanical models

Biomechanical models of strabismus are homeomorphic models that focus on the globe, connective tissues, extraocular muscles, and innervations. The first biomechanical models were the familiar ophthalmotropes of Ruete, Wundt and others (Ruete, 1857; Wundt, 1862). Computer models have a critical advantage over the old ophthalmotropes in that their behavior is constrained only by our understanding of extraocular biomechanics, and not by the materials and mechanisms feasible in a table-top physical model.

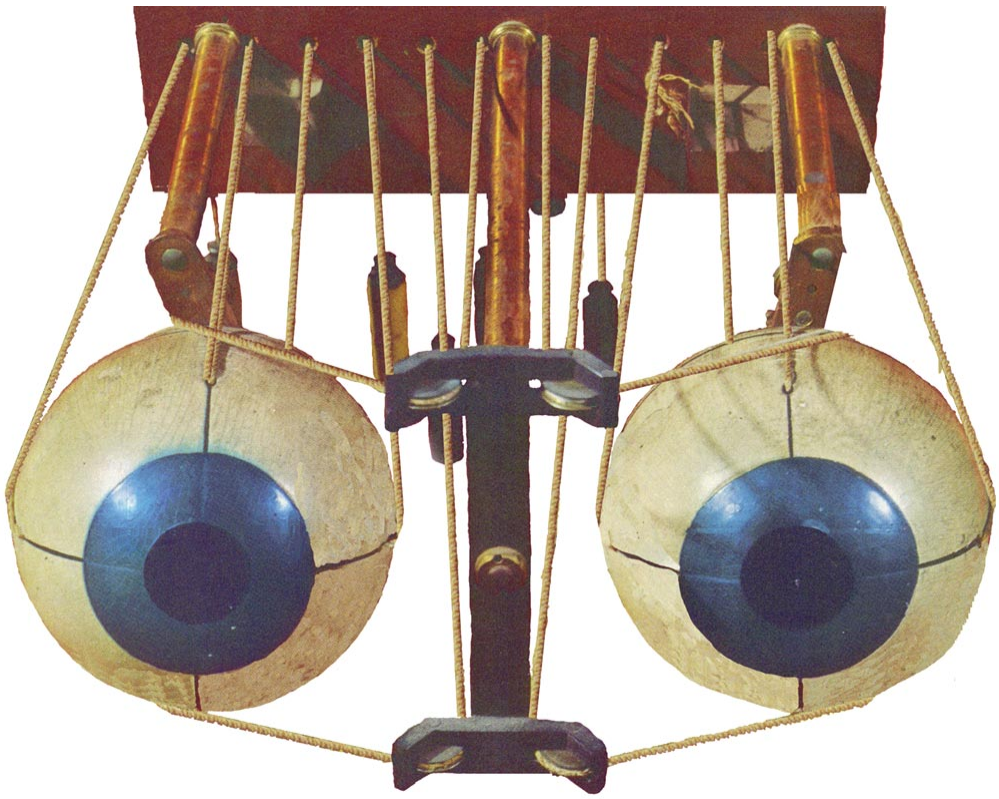

Figure 7-1. *Knapp's 1861 ball and string ophthalmotrope reflects only extraocular geometry, ignoring contractile and elastic tissue properties and coordination of innervations.*

Biomechanical models assume that the complex behavior of muscles (Partridge and Benton, 1982) can be understood in terms of simple arrangements of elastic and force-generating elements; that complex orbital connective tissues can be represented by simpler elasticities; and that the orbital contents can be analyzed in isolation from the rest of the organism. Little attention is paid to non-mechanical factors, not because they are unimportant, but because they are largely separable from the mechanics. In any case, non-mechanical factors must act through the eyes' mechanics. Thus, understanding extraocular mechanics facilitates, by "subtraction", the study of non-mechanical factors.

Orbital geometry, muscle and connective tissue mechanics, and innervations are intertwined in ways that generally cannot be understood without a model of orbital biomechanics. Robinson (Robinson, 1975) laid a foundation for biomechanical models of ocular alignment with a system of equations and computational procedures, based on balancing the static forces of extraocular muscles and orbital tissues, and oriented to simulate strabismic disorders and their surgical correction. Variation in tension across the width of muscles (Miller and Robinson, 1984), and Lockwood's ligament, an elastic connection between the inferior rectus (IR) and inferior oblique (IO) (Kusel and Haase, 1977; Günther, et al, 1986) have been modeled. The Robinson model has been tested against clinical data (Clement, 1982; Clement, 1985; Clement and Howrie, 1985; Howrie and Clement, 1986), Miller and Robinson (Miller and Robinson, 1984), provided muscles with

innervation-length-tension relationships having "slack" and "leash" regions, made muscle sideslip a function of tension, allowed globe translation, and provided full binocularity. This computational model was called SQUINT.

There are two modern models derived from this line of work. Simonsz (Simonsz and Spekreijse, 1996) reviewed much of the existing data on orbital geometry and tissue stiffness, and conducted several new studies to develop a model that runs on a “palmtop” computer, achieving simplicity of use, rapidity of calculation, and clinical utility by limiting abnormalities and manipulations to eye size, muscle origins, insertions, length-tension relationships, and innervations. The second model is a Macintosh™ application called Orbit™,(Miller, et al, 1996) which incorporates and provides a user-friendly interface to SQUINT, hiding much of SQUINT’s complexity instead of restricting its generality. The National Institutes of Health / National Eye Institute (NIH / NEI) has continued to support SQUINT development, and the physiologic research on which it is based.

Physiologic Basis

A biomechanical model in isolation is only an academic exercise. But, with strong links to physiologic research, a biomechanical strabismus model can have both clinical utility and scientific validity. As a *clinical tool*, it can help assimilate patient data, aiding diagnoses, and clarifying treatment possibilities. As a scientific *theory* or *hypothesis*, such models propose explanations of normal and abnormal binocular alignment. Both roles cast the model as a construction or abstraction based on various kinds of data (inward pointing arrows of figure 7-2). Equally important is a model’s role in influencing where investigators look for relevant data , and what tools they use (Feyerabend, 1988). Biomechanical strabismus models have been particularly fruitful in this regard (outward pointing arrows of figure 7-2). In particular, the failure of early strabismus models to predict outcomes of transposition surgeries led to the concept of *extraocular muscle pulleys* (Miller and Demer, 1992), and testing that concept by magnetic resonance imaging (MRI) before and after transposition surgery (figure 7-2, lower right panel).

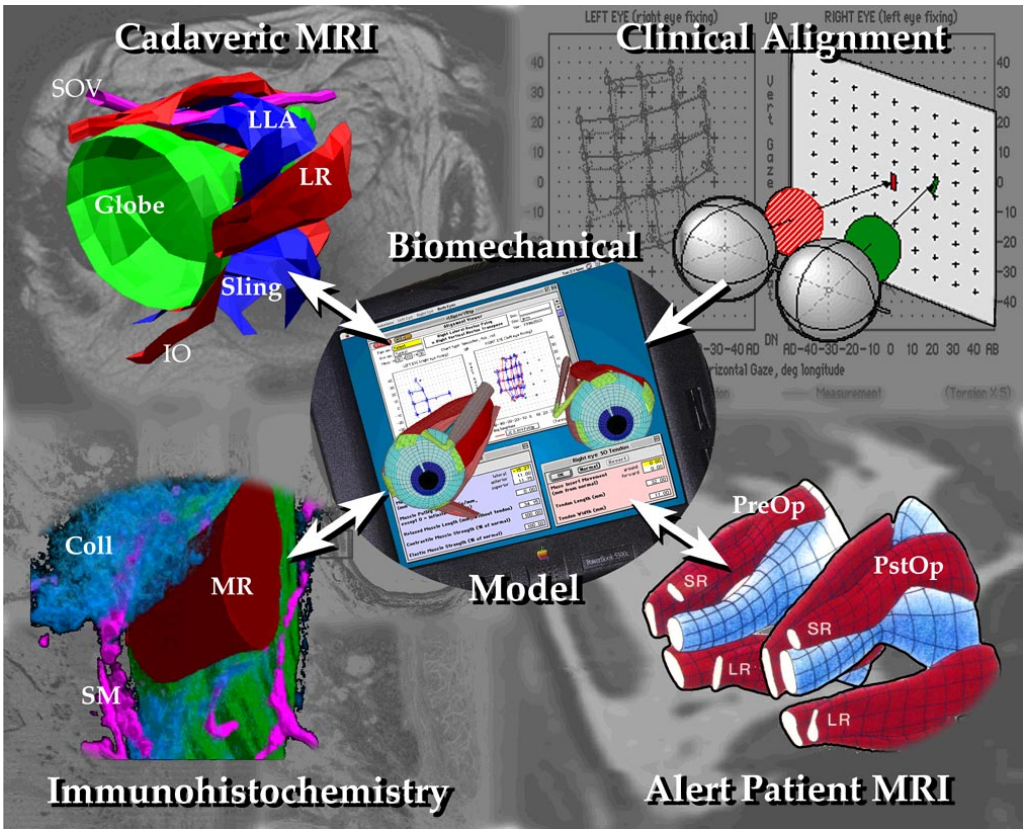

Figure 7-2. *Some Types of Data Expressible in a Biomechanical Model.* Inward-pointing arrows *indicate data that are incorporated into a model.* Outward-pointing arrows *indicate studies suggested by modeling.* ***Cadaveric MRI*** *studies can take advantage of long scan times to give near-microscopic resolution of connective tissue planes.* SOV *= sup orbital vein,* Globe *= globe & optic nerve,* Sling *= posterior sling portion of lateral rectus (LR) pulley.* ***Clinical Alignment*** *data are compared with model predictions.* ***Immunohistochemistry*** *identifies specific tissue types. Thin slices are then digitized and reconstructed to restore 3D tissue relationships. Region of medial rectus (MR) pulley is shown, with a quadrant of Coll = collagen (blue) removed to reveal* SM *= smooth muscle (pink).* ***Alert Patient MRI*** *studies were initially used to establish normal functional anatomy (Miller, 1989) and are now used to study anatomic and contractile abnormalities and effects of surgery (Demer and Kerman, 1994; Demer, et al, 1994; Demer and Miller, 1995; Demer, et al, 1995a; Demer and Miller, 1997). Pre-* (PreOP) *and post-operative* (PstOp) *scans are shown for a case of LR palsy treated by vertical rectus transposition. The belly of the transposed superior rectus (SR) resists lateral pull of the transposed insertion.*

Extraocular imaging

Muscle forces and axes of rotation are central variables in biomechanical strabismus models. A muscle's axis of rotation gives the direction in which it tends to spin the globe; and the muscle force gives the magnitude of that tendency. Modern extraocular imaging was motivated by modelers' needs for accurate descriptions of muscle paths, the determinants of those paths, and muscle cross-sections and contractilities (Robinson, 1975; Miller, 1984; Miller, 1985; Miller and Demer, 1992; Miller, et al, 1993). We used MRI to demonstrate that the paths of rectus muscle bellies are stable in the orbit throughout the oculomotor range (Miller, 1989), and showed that MRI can estimate EOM contractility and atrophy (Miller, 1989; Demer, et al, 1994; Demer and Miller, 1995). Below, we analyze a case that had been diagnosed as oblique muscle dysfunction, in which MRI demonstrated normal oblique muscle contractilities and cross-sections (Clark, et al, 1997b). Extraocular imaging is the focus of Chapter 6.

Immunohistochemistry and electron microscopy

In vitro study of extraocular tissues has provided histologic and structural details to supplement *in vivo* imaging. Human cadaveric orbits were de-calcified, imbedded in paraffin, and cut in 10μ sections. Three interleaved sets of sections were treated with Masson's Trichrome stain, which visualizes muscle and collagen, an immunohistochemical stain for smooth muscle alpha actin, and van Gieson's elastin stain, respectively. Slices were mounted and digitally photographed for computer reconstruction (figure 7-3).

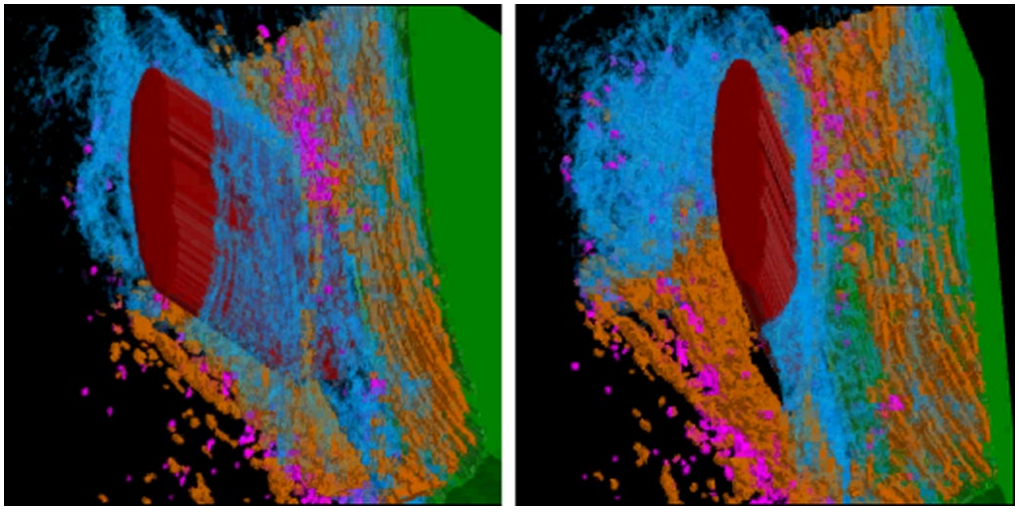

Figure 7-3. Anterior MR Showing Collagen, Elastin & Smooth Muscle. Computer reconstruction is shown from two posterior-inferior perspectives (some readers will be able to fuse the two images as a crossed-disparity stereogram). The MR (brick red) with cut posterior edge, and a piece of the globe (green) are shown. So that other structures would be visible, we decimated the collagen (blue), rendered it translucent, and deleted its inferior-medial quadrant. Thus, collagen is actually denser than shown. For clarity, only the highest densities of elastin (orange) are shown. Elastin encircles the

MR. A band of smooth muscle (pink) also encircles the MR, and is particularly dense between the MR and the orbital wall, perhaps serving to control the coupling of the MR to the orbital wall. (QuickTime®, VR movies of this and other reconstructions are available at Internet address http://www.ski.org/JMMiller_lab/OTA_proj.)

Perhaps the most interesting result of these immunohistochemical studies is the prevalence of smooth muscle cells in the connective tissue around the rectus EOMs in the vicinity of the globe equator (constituting what was called by an anonymous NEI grant reviewer "innervated connective tissue"). This smooth muscle helps reconcile the existence of mechanically significant connective tissue constraints on muscle path, with the informal intrasurgical observation that EOM bellies do not seem firmly fixed to the orbit. We have since traced a sympathetic projection to midorbital smooth muscle from the ipsilateral superior cervical ganglion, and have found evidence of parasympathetic innervation (Demer, et al, 1995c; Demer, et al, 1997).

Further evidence that these tissues function to control muscle path comes from electron microscopy, which shows pulley collagen to be extremely dense and organized in an unusual, crisscrossed configuration suited to high internal rigidity (Porter, et al, 1995; Porter, et al, 1996). On the basis of these studies, we have created an overall scheme of human extraocular connective tissue (Demer, et al, 1995b; Demer, et al, 1996); figure 7-4).

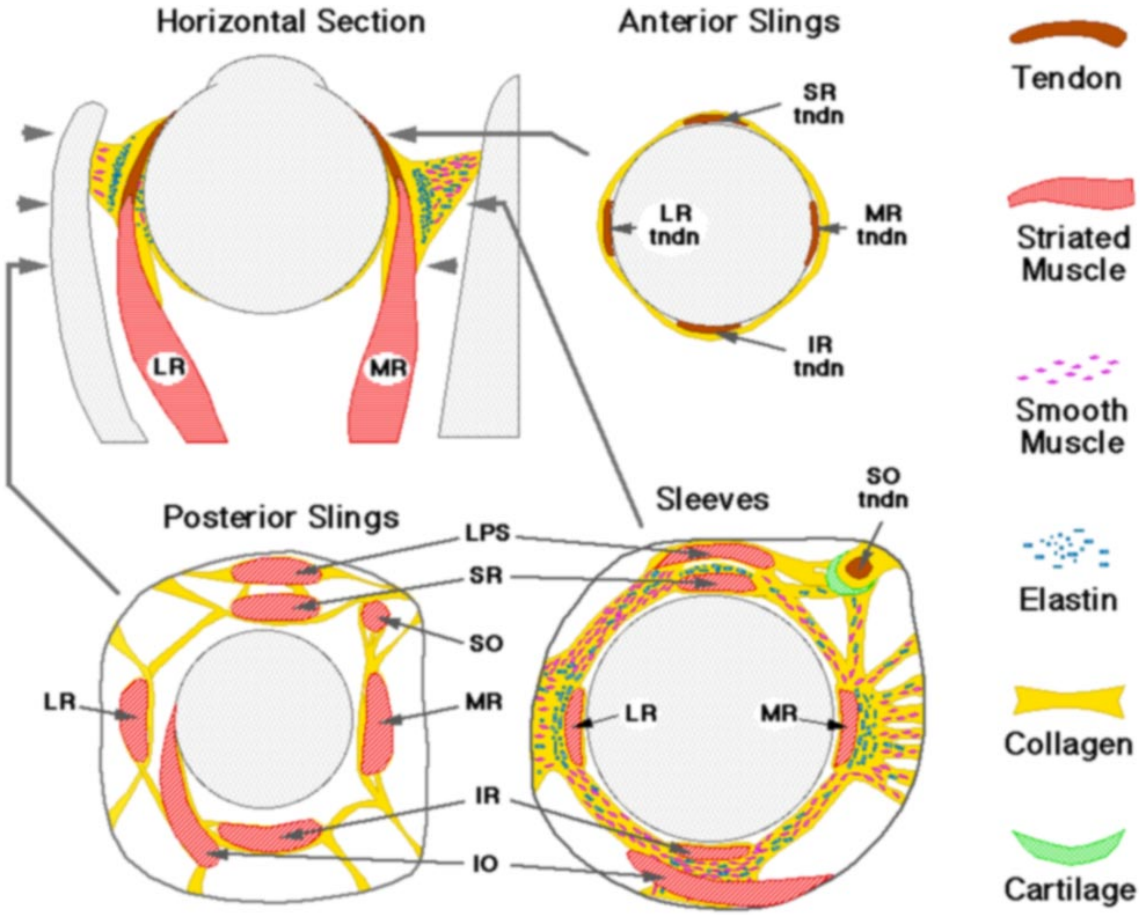

Figure 7-4. *Diagrammatic representation of structure of orbital connective tissues.* IR - *inferior rectus.* LPS - *levator palpebrae superioris.* LR - *lateral rectus.* MR - *medial rectus.* SO - *superior oblique.* SR - *superior rectus. Coronal views represented at levels indicated by arrows in* Horizontal Section.

Rectus muscle pulleys

From the complex arrangement of tissues diagrammed in Figure 7-4, we developed the concept of *muscle pulleys.* A muscle pulley consists of a ring or sleeve of collagen, elastin and smooth muscle, encircling an EOM, and coupled to the orbital wall and other connective tissue structures by bands of collagen, elastin, and smooth muscle. Tendons and muscles travel through pulleys by sliding inside thin collagenous sheaths that telescope within the pulley sleeves. The pulleys are fixed relative to the orbit, and in straight ahead gaze are located near the globe equator in Tenon's fascia (Demer, et al, 1995b; Demer, et al, 1996).

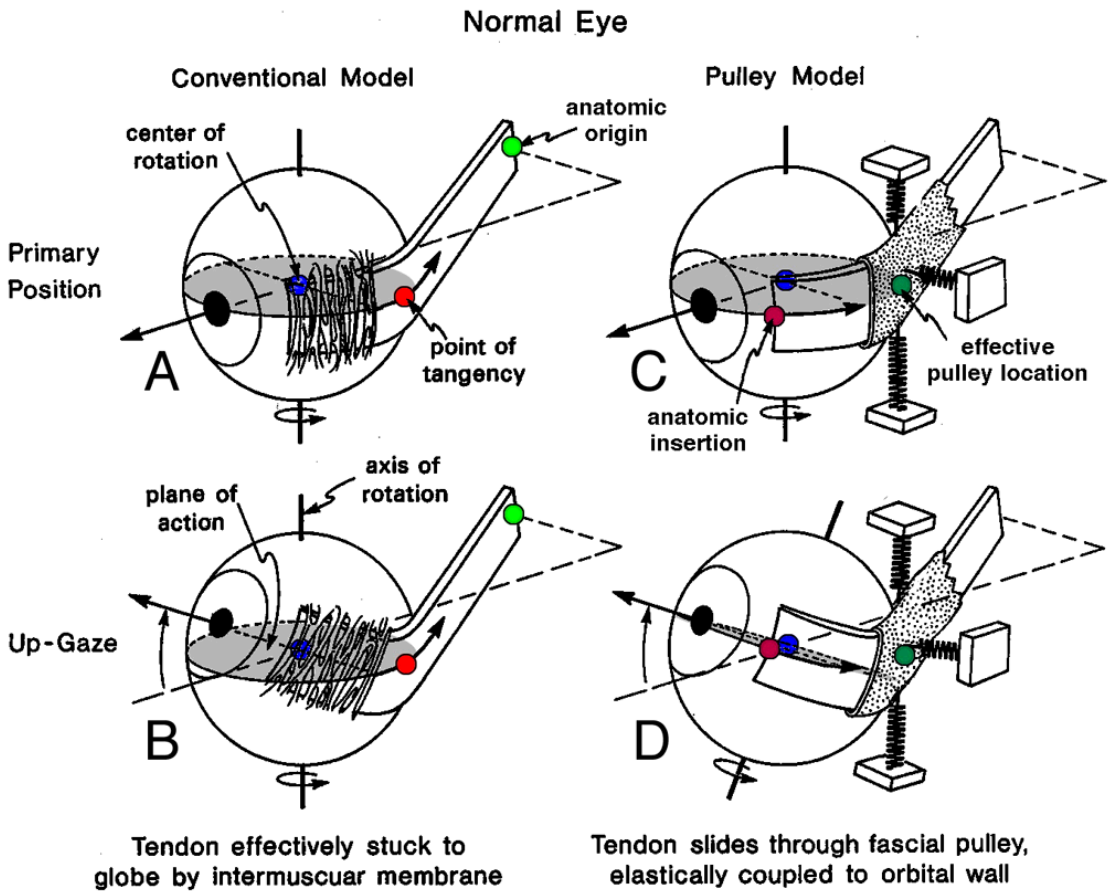

Figure 7-5. *Muscle actions differ in conventional and pulley models. A muscle's* axis of rotation *(indicated by "spin" arrows) is the axis the eye tends to rotate about when the muscle contracts.* ***A & B:*** *In a* conventional *model, the muscle acts as though it were inserted at its point of tangency with the globe. In elevation, it is as though there were a hinge at this point, and the axis of rotation remains roughly fixed with respect to the orbit.* ***C & D:*** *In a* pulley *model, the muscle passes through a connective tissue pulley that is stabilized with respect to the orbital wall, and determines the effective muscle origin. In elevation, the axis of rotation tilts with the eye. Note that muscle paths can be the same in the two models, although mechanical actions are different.*

Pulleys have important implications for EOM function. Whereas the direction of pull (or axis of rotation) of an EOM was once thought to be determined by its anatomic origin in the annulus of Zinn (along with its point of tangency with the globe and the globe center), according to the pulley model the *functional origin* of an EOM is its pulley. The path length of an EOM, which determines its stretch, and therefore its tension, is increased by deflection through the pulley. Despite being stiffened by elastin, pulleys are compliant and potentially subject to actions of their suspensory smooth muscles, as well as changes in EOM tension (Clark, et al, 1997a). Although no functional role of pulley smooth muscle is proven, several roles are plausible. The smooth muscles might simply increase the

stiffness of Tenon's fascia and the pulley suspensions to provide a constant load and geometry for the ocular motor system. Simulation shows that binocular alignment is highly sensitive to pulley position (Clark, et al, 1997b). Thus, it is possible to imagine that smooth muscle tension is modulated to refine binocular alignment or assist in slow eye movements such as convergence.

Binocular alignment measurements

Alignment data routinely collected in the clinic is often not useful for modeling. The following are guidelines for collecting quantitatively useful data:

- Eyes must be completely dissociated, with fixing and following eyes specified and controlled.

- Fixing eye gaze angles must be specified. Thus, target positions must be defined, and patient head position controlled.

- Include a sufficient number of gaze angles over a large enough field to reasonably constrain the simulation. Clinical data is modeled by adjusting model parameters to fit—if there is insufficient data, many different sets of model parameters (corresponding to different diagnoses) may fit the data, so that modeling is indeterminate. If the range of fixation is too small, distinguishing features of the pattern of misalignment (deviation) will not appear in the data. We routinely collect data for 21 fixations with each eye over a ±30° x ±30° field. Nine fixation points might be considered a minimum.

The Clement Clark Electric Hess Screen (Figure 7-6; Harlow, England) is convenient to use, and adequate in the above respects.

- Try to measure objective torsion. Torsion is simply the third coordinate (with horizontal and vertical angles) needed to specify eye rotation, and measuring it provides more data to constrain modeling. Torsional measurements may be of particular use in discriminating oblique muscle disorders. Unfortunately, subjective torsion measurements may be unstable, and it may be unclear which is the torted eye. Objective measures (e.g., ophthalmoscopy or fundus photography) in non-primary positions may be inconvenient to obtain in the clinic.

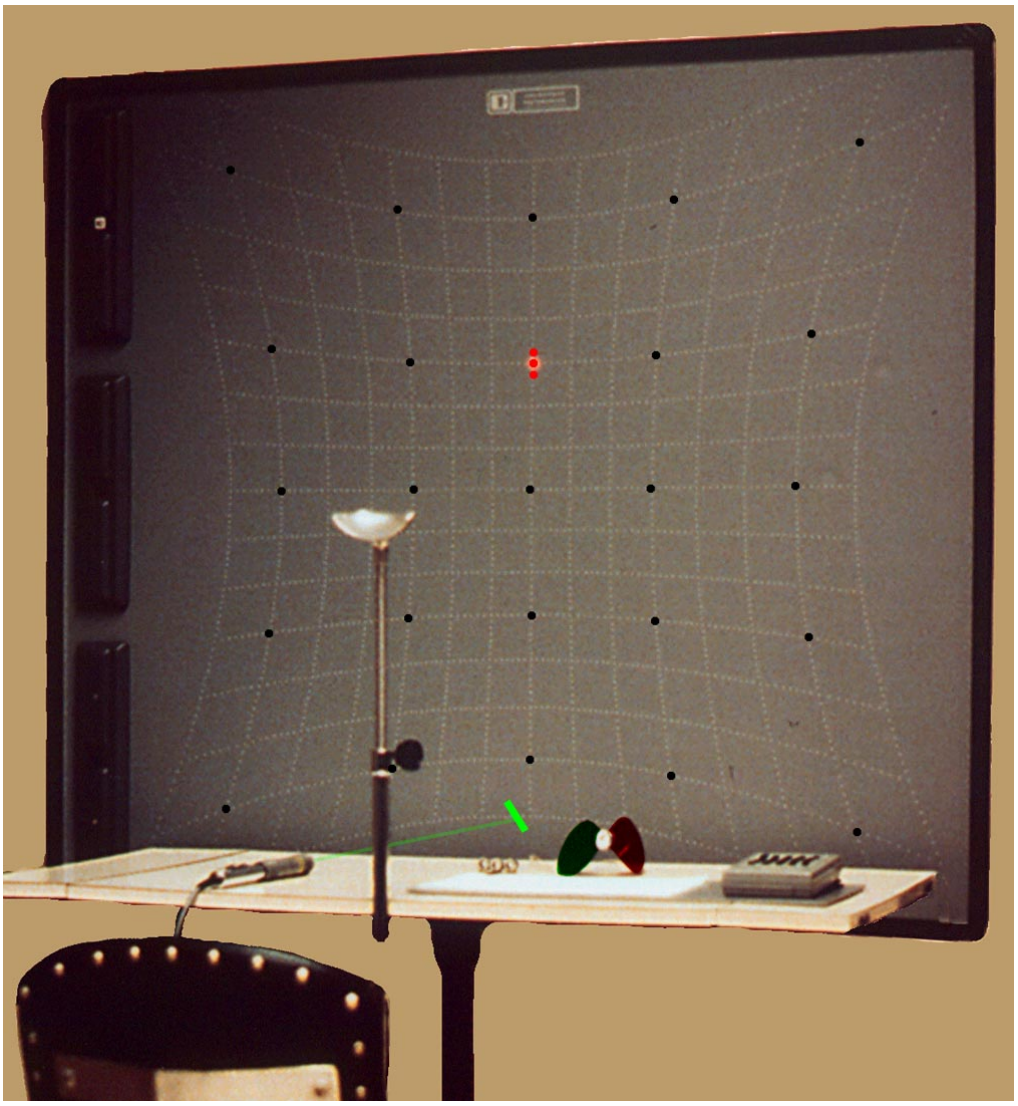

Figure 7-6. *A Clement-Clark Electric Hess Screen, modified to replace each red fixation LED with a vertical row of three LEDs, allowing measurement of ocular torsion. The subject sits with chin (and, if necessary, forehead) stabilized against a support 50 cm from the screen. Eyes are dissociated with red and green filter goggles. The subject indicates localizations using a hand-held green streak projector.*

Clinical Applications

When Is A Biomechanical Model Useful In Treatment Planning?

We compared predictions of the Orbit model with published surgical dose recommendations for comitant esotropia and exotropia, and found that model predictions agreed with published recommendations (Park, et al, 1996). Interestingly, modeling showed that these simple types of horizontal strabismus responded to surgery independent of their mechanical, innervational, or combined etiology, surely part of the reason for the broad success of the recommendations. This illustrates how modeling can be used to clarify traditional methods, a laudable scientific goal, but also shows that there is little reason to use a biomechanical model with simple, familiar types of strabismus—traditional tables supplemented by clinical judgment are sufficient.

How to Use a Biomechanical Model in Diagnosis

Modeling has three steps:

1. Simulate the preoperative disorder.
2. Apply surgical manipulations to the preoperative simulation.
3. Compare simulated and actual surgical outcomes.

One can ask many questions of a strabismus model—what are the muscle forces? Innervations? Muscle paths? —and compare these predictions to measured or desired values. In strabismus management, binocular alignment is usually of central concern, and so we usually compare predictions and measurements of alignment. Thus the Orbit model is designed to predict results of a dissociated eye alignment test, such as the Hess, Lancaster, or prism-cover test. We use a format similar to that of the Hess and Lancaster tests, which shows *intended gaze* (the gaze angles of the *fixing eye*, reflected across the midline), positions of the *following eye* (the eye moving passively under the innervations determined by the fixing eye), and the overall pattern of misalignment (deviation), for 21 positions over a ±30° x ±30° field (see, e.g., figure 7-7).

Hundreds of parameters are needed to describe the anatomy and physiology of the eyes, but it is impractical to measure more than a few of them in a given patient. Such situations, familiar in the life sciences, require a *normative assumption*, that is, a patient is assumed normal, except where there is evidence to the contrary. Thus, we begin a simulation with a description of normal eyes, based on physiologic studies, such as those described above. An alignment chart for normal eyes is shown in figure 7-7.

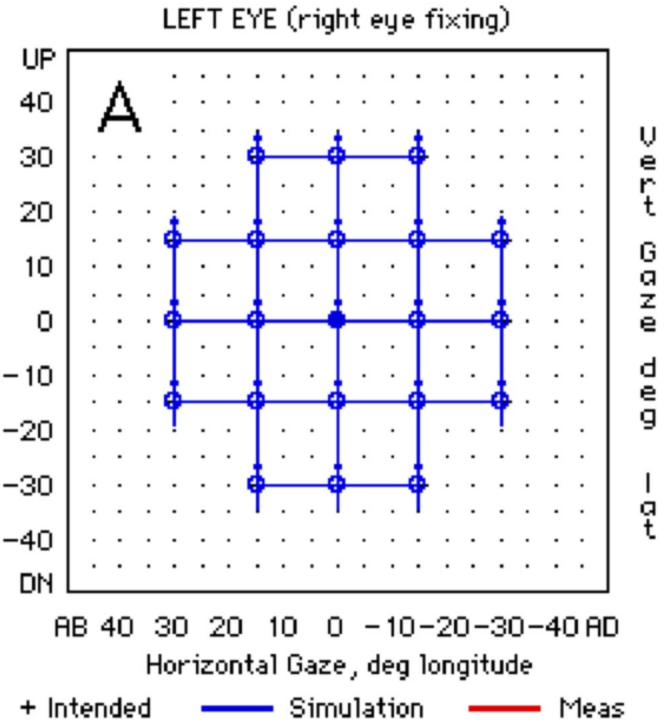

Figure 7-7. *Alignment of left eye (right eye fixing), Starting simulation, which assumes eyes are normal.* Intended gaze angles *are hidden by simulated positions of the left* following eye*(°), which fall directly on top. Arrows through the circles show torsion, with the angle from straight up indicating abnormal torsion (torsion in excess of that prescribed by Listing's Law), multiplied by 5 in the figure for visibility. Following eye positions are connected by grid lines to clarify the correspondence of following and intended positions, and to emphasize the alignment pattern.*

To demonstrate modeling procedures consider Patient AT, a 19 year old white male who suffered whiplash, wrist and chest injuries, but no direct head injury or loss of consciousness, in an automobile collision. During recovery, he developed incomitant left hypertropia of 3° (6 pd) in left gaze, increasing to 17° (30 pd) in right down gaze, and right head tilt of 7-10°. Excyclotorsion of 6° was measured by double Maddox rods. A forced head tilt test to the left was strongly positive. Left superior oblique (SO) palsy was diagnosed.

Figure 7-8A shows AT's preoperative alignment data, slightly smoothed to help focus on general modeling principles, rather than case idiosyncrasies. Actual cases of strabismus often involve secondary muscular and innervational changes. Subjective measurements of torsion are shown, but because of their unreliability, we only consider them informally.

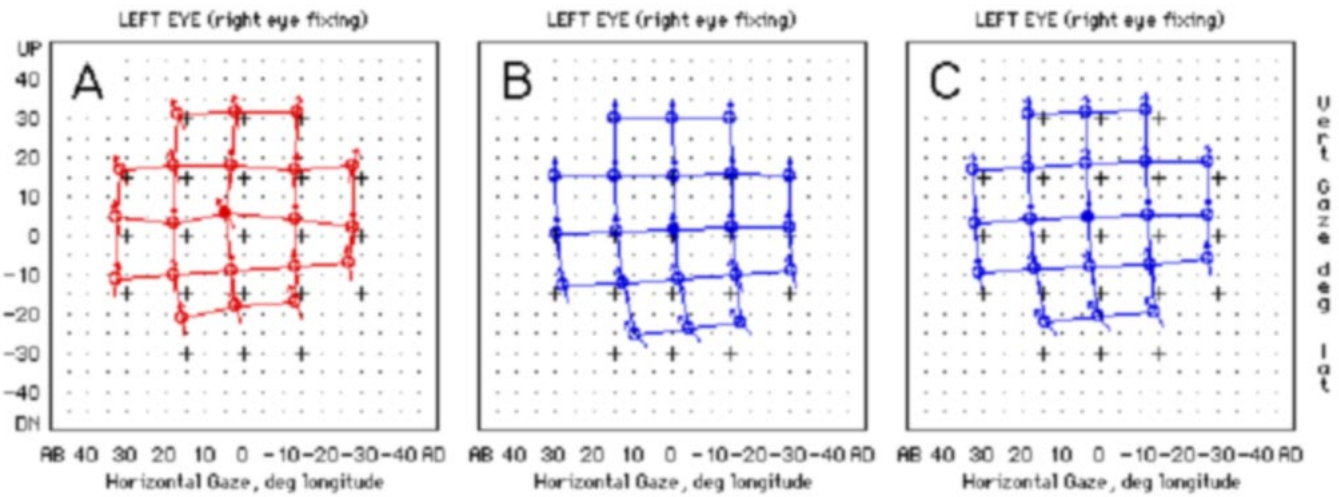

Figure 7-8. *Patient AT, preoperative alignment of left eye (ie, left eye following, right eye fixing),* ***A:*** *Idealized preoperative binocular alignment data. Figure shows* intended gaze angles *for the left eye (+), determined by the positions of the right fixing eye, and measured positions of the left eye (o).* ***B:*** *Preliminary simulated preoperative alignment with left SO contractile force set to zero. There are systematic differences between this simulation and the data of panel A.* ***C:*** *Final simulated preoperative alignment, with left SO contractile muscle force zero, reflecting paralysis, elastic muscle force at 50% normal, reflecting atrophy, and small adjustments of LR, MR, and SR muscle lengths.*

We begin analysis with simulated normal eyes (figure 7-7). The aim of preoperative simulation is to bring simulated eye alignment into congruence with the clinical data (figure 7-8A). What is the biomechanical mechanism of the " SO palsy" of figure 7-8A; is it simply that the left SO fails to contract, or is there more?

Contractile muscle force (developed force) is produced under control of innervation. Interpreting the diagnosis literally, we suppose that left SO contractile force is zero (we enter "0" in the appropriate place in the model). The model predicts preoperative alignment shown in figure 7-8B. Although this preliminary simulation captures some features of the clinical data (figure 7-8A), including limitation of downgaze, particularly in adduction, and excyclorotation, particularly in downgaze, magnitudes are systematically different from the data of 7-8A. Thus, we do not yet have an adequate simulation of the patient's preoperative disorder.

What else do we know or suspect about AT's disorder? Here, modeling is similar to traditional diagnosis: if we have test results, we use them; otherwise we proceed on general experience or hypothesis. Here, we suspect that the denervated LSO has become atrophic, that is, its *elastic force* is subnormal, as well as its contractile force. If appropriate orbital images were available, we could estimate the reduction in elastic force by comparing the cross-sectional area of the paretic left SO with that of the normal right SO (Demer and Miller, 1995). We could also verify our contractile force assumption, as

described in Chapter 6. However, MRI data were not available in this case, so on the basis of experience with similar cases, we suppose that LSO elastic strength is 50% of normal. Running the modified simulation gives a good match to clinical data, except for small horizontal and vertical offsets of the entire alignment pattern. We suppose that these are due to small, almost negligible, abnormalities in rectus muscle lengths, either idiosyncratic, or secondary to the palsy. Thus, we make some adjustments (~1 mm) in LR, MR, and SR muscle lengths. Figure 7-8C shows the resulting simulation, which is a good match to AT's clinical alignment pattern.

We now have a reasonable simulation of Patient AT's preoperative strabismus, which is also a biomechanical diagnosis: AT's left SO is denervated and has atrophied—it develops no contractile force, and only half of normal elastic force. Everything else, including AT's right eye, is normal or close to it. Modeling shows the *implications* of our hypotheses: that, in this case, SO palsy with atrophy, and slightly abnormal rectus muscle lengths can account for the patient's binocular misalignment. The preoperative simulation also serves as the starting point for treatment analysis.

Treatment Simulation

A year and a half after Patient AT's accident, he underwent strabismus surgery. Measured and simulated postoperative alignment are shown in figure 7-9. In both the patient and the model, the left IO was moved 5 mm posterior to the temporal insertion of the IR and 1 mm temporal to it, and the right IR was recessed 4.5 mm.

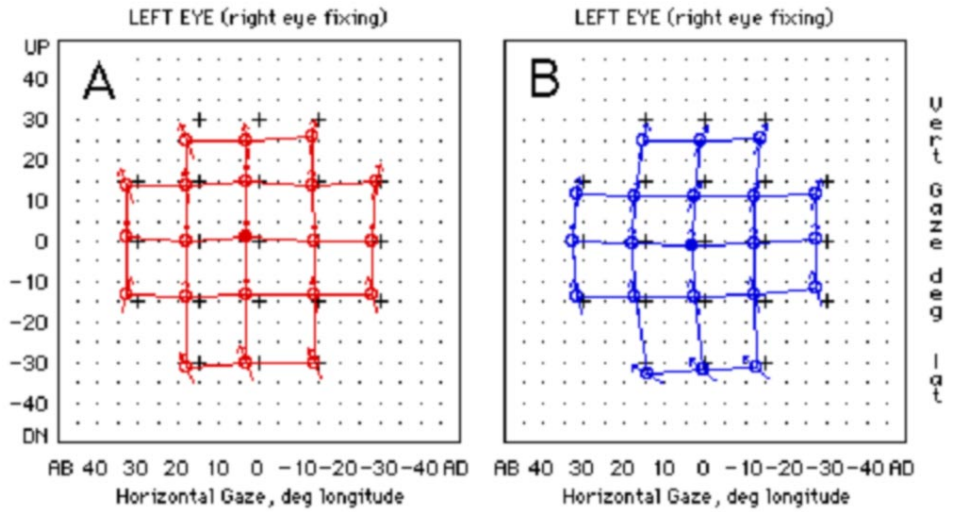

Figure 7-9. *Patient AT, postoperative alignment of left eye (right eye fixing).* ***A:*** *Postoperative clinical data.* ***B:*** *Simulated postoperative alignment. The fit is good, showing that the model accurately predicts surgical outcome, and, indirectly, that our pre-op simulation (Figure 7-8C) was reasonable.*

It can be seen that the simulation was a good predictor of surgical outcome. One month postoperatively, AT no longer reported diplopia, and alignment was orthotropic, except for a small, asymptomatic right hypertropia in extreme right upgaze.

Role in Teaching and Changing Patterns of Clinical Practice

Schools of thought

The philosopher of science Thomas Kuhn(Kuhn, 1970) described a pre-scientific stage in which, lacking a unifying scheme of thought, or *paradigm*, practitioners in a field form intellectual alliances—*schools of thought*— around prominent teachers or doctrines. Discussion and debate at the schools-of-thought stage consist mainly of appeals to authority. Science emerges with the general acceptance of a paradigm, in terms of which further scientific evolution is articulated and evaluated.

A unifying framework for theory and practice in strabismus

We know of only one approach that might emerge as a paradigm for strabismus, and although most would probably agree that biomechanics may ultimately be the correct way to analyze binocular alignment, many argue that complexities of extraocular architecture, vagaries of post-traumatic and post-surgical healing, plasticity of central innervation, and individual differences, would make such analyses impractical. We have already touched on some ways in which modeling has driven studies that have clarified extraocular architecture (figure 7-3). Biomechanical effects of healing can similarly be studied. Central plasticity can be studied with the help of an extraocular model to infer changes in innervation that would account for observed changes in alignment. Individual differences present problems that will need to be addressed on several fronts. First, tomographic imaging can provide indices of EOM elasticity and contractility, and also, of orbit and globe anomalies that affect extraocular geometry (see Chapter 6). Some features of extraocular connective tissue can be inferred from images of EOM paths as a function of gaze (Clark, et al, 1997a). Second, characterization of extraocular parameters by gender, race, and age would account for some of the variations between patients.

Patterns of specialization and referral evolved in an era in which human health was thought priceless, will surely change. It will become more difficult to justify costs of sending patients to distant experts, and so local specialists, ideally in consultation with experts, will become responsible for more sophisticated diagnoses and treatments. Instead of moving patients to experts, expertise will be brought to local specialists. Without accurate communication, however, it will be difficult for remote experts to provide more than hints. Accurate communication and precise definition of terms are also necessary for multi-center clinical trials of new approaches in strabismus.

If patient data is to be shared, quantification must be well-defined. Do all clinicians mean the same thing by “minus 3 gaze limitation?” Even with alignment measurements, quantification may be nominal, e.g., deviations by prism-cover test do not typically specify the intended gaze angle at which non-primary deviations were measured, or even which eye looked through the prisms. Well-defined quantification is essential for biomechanical modeling, and for reliable communication.

Strabismus nomenclature is an ill-defined mixture of terms like “hypertropia” and “V-pattern.” which describe symptoms (observations), and terms like “underaction,”

“overaction,” and “contracture,” which sound etiologic, as though they point to mechanisms underlying observations, but usually are just alternative descriptions of symptoms. Etiologic terms may seem convenient descriptions of complex observations, for instance, “superior oblique palsy” used to mean “limited depression and excyclorotation, particularly in adduction,” but they become barriers to clear thinking in such cases where e.g., the superior oblique muscle is perfectly normal (Clark, et al, 1997b). Biomechanical modeling can help by defining precise etiologic terms, distinguishing, for example, contractile muscle strength, elastic muscle strength, and relaxed muscle length, which have different effects on motility, not distinguished by referring to “weak” and “strong” muscles.

Case Studies

Heterotopic pulleys & pattern strabismus

"A" pattern strabismus is horizontal strabismus in which the eyes are relatively diverged in downgaze (or relatively converged in upgaze). “A” patterns are usually attributed to oblique muscle dysfunction. However, simulation shows that significant displacement of rectus muscle pulleys, that is, heterotopic pulleys, can also produce “A” patterns (Clark, et al, 1997b).

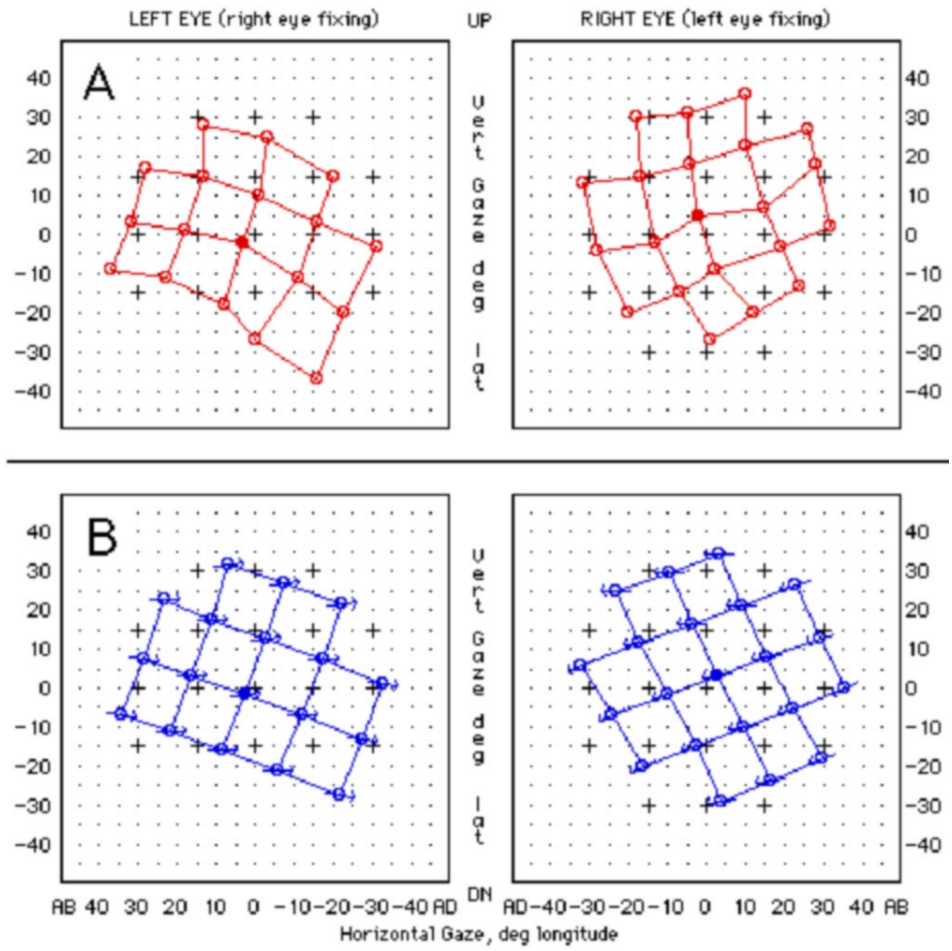

Figure 7-10. *Patient TL, binocular alignment prior to strabismus surgery.* ***A:*** *A-pattern clinical binocular alignment measurements.* ***B:*** *Simulated misalignment due to TL's heterotopic pulleys, with eyes otherwise normal.* ***Left panels*** *show positions of left eye with right eye fixing, and* ***right panels,*** *positions of right eye with left eye fixing.*

Patient TL has "A" pattern strabismus, which might be attributed to "overacting superior obliques" (figure 7-10A). However, coronal MRI shows clear pulley heterotopy (figure 7-11), and simulation shows that this pulley disorder can account for the pattern of misalignment (figure 7-10B). .

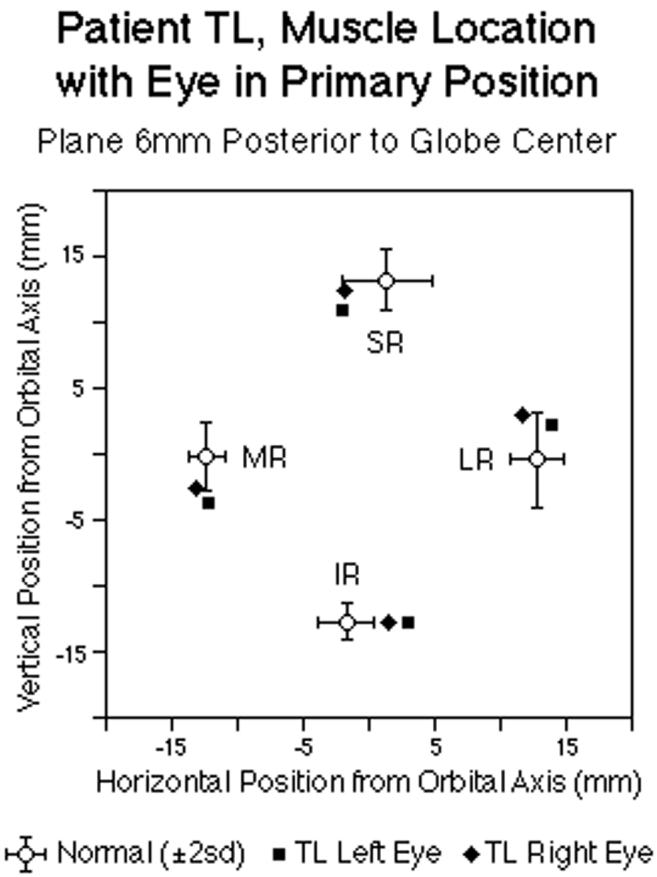

Figure 7-11. *Coronal MRI scan of patient TL at a level 5 mm posterior to the globe center. Pulleys are located at the centroids of the outlined rectus muscles. Dots show normal pulley locations. Normal pulley positions are derived from 10 orbits in 6 subjects.*

We have identified significant pulley heterotopy in 11 of 12 patients studied so far with "A" or "V" pattern strabismus. Simulations are consistent with the idea that abnormal rectus pulling directions due to pulley displacements can cause or contribute to misalignments typically diagnosed as oblique muscle over- or underactions (Clark, et al, 1997b). This insight has been useful in avoiding futile surgeries on oblique muscles (Demer, et al, 1992).

It has been suggested that abnormal rectus pulley positions might be a result of torsional malposition of the eyes (Guyton and Weingarten, 1994). While we cannot rule out this hypothesis in all cases, evaluation of pulley positions in 14 orbits of 7 excyclotropic subjects with SO palsy confirmed by MRI showed that the only significant pulley abnormality was MR pulley elevation by an average of 1.1 mm (Clark, et al, 1997b). An Isolated pulley displacement could not be the result of ocular torsion, particularly because the MR pulley has the firmest coupling to the orbital wall . Perhaps the upward displacement of the MR is due to movement into the space made by loss or atrophy of the adjacent SO.

Vertical rectus transposition with posterior augmentation sutures

Since at least the 1970's, conventional vertical rectus transposition for LR palsy has been augmented with posterior sutures, pulling the lateral borders of the transposed superior and inferior recti to the borders of the paralyzed LR , although only recently has this procedure been analyzed and published (Foster, 1997). Orbit ™ simulations provided an analysis of the procedure's success in increasing horizontal range of gaze with little loss of vertical range. Postoperative MRI scans show clear inflections in the paths of transposed EOMs at locations that approximate pulley locations demonstrated grossly and histologically (figure 7-12B) (Demer, et al, 1995b; Clark, et al, 1997a).

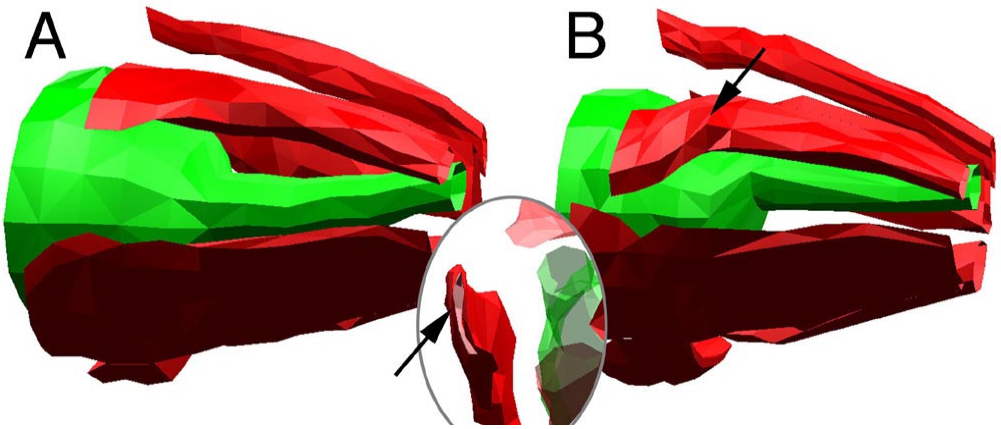

Figure 7-12. *Patient TS, 3-D MRI reconstructions of extraocular muscle paths in primary gaze.* ***A:*** *Preoperative MRI scan shows left SO and left LR atrophy typical of chronic denervation. Note in inset, posterior view showing unusually thin LR.* ***B:*** *Postoperative MRI shows little lateral displacement of SR and IR belly (not shown in this view), with marked path inflections (arrow to SR) as muscles course through pulleys to their transposed insertions.*

Patient TS, a 33 year old white male, experienced horizontal diplopia prior to surgical resection of a chordoma, and both horizontal and vertical diplopia after. The tumor enveloped the abducens nerve, which was almost certainly lost to the resection. Within 2 weeks, TS adopted a left face turn of 10-15°. Left eye abducting saccades were slowed to less than 100°/sec (saccades in other directions were normal). Binocular alignment was as shown in Figure 7-13A: incomitant left esotropia greatest in left gaze, a large secondary deviation with the left eye fixating, and a "V" pattern characteristic of SO palsy. MRI scans performed the same day as the alignment measurements are shown in figure 7-12A (3D reconstruction) and figure 7-14A.

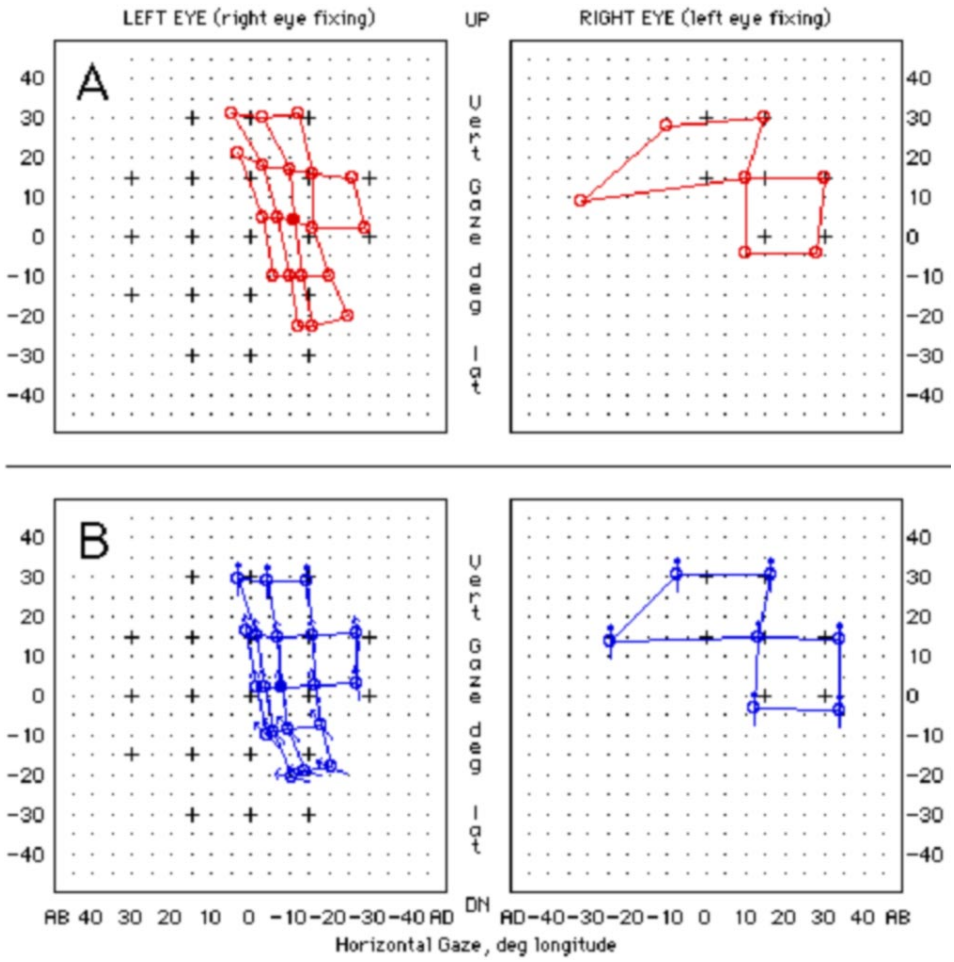

Figure 7-13. *Patient TS, binocular alignment after chordoma resection, but before strabismus surgery.* ***A:*** *Clinical measurements. Left eye shows severely limited abduction characteristic of left LR palsy, and "V" pattern, characteristic of left SO palsy. Right eye shows a large secondary deviation. Only a few right eye positions could be measured because of the limited left eye fixation range.* ***B:*** *Simulation (described in text) is a good representation of measurements.*

To simulate TS's strabismus, from the MRI data of figure 7-14A, left LR contractile strength is reduced to zero and left LR elastic strength to 25% of normal. These changes reflect that the abducens nerve was lost and that marked left LR atrophy followed. Also from the MRI data, left SO contractility is set to 0, and left MR contractility to 50% of normal. These impairments may reflect collateral damage of chordoma surgery. The resulting simulation is a good match to the preoperative clinical measurements, as shown in Figure 7-13B.

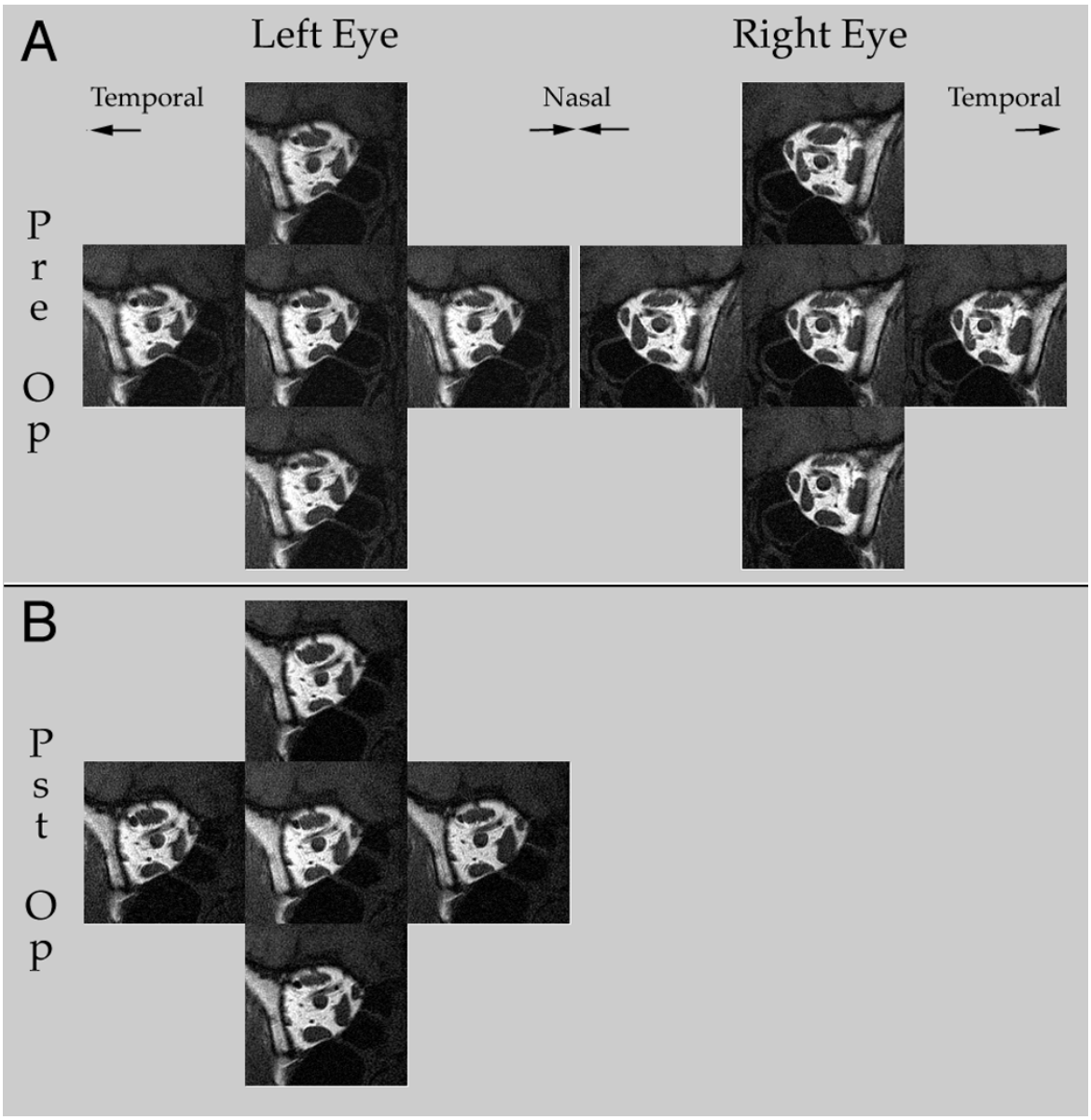

Figure 7-14. *Patient TS, fixing along the orbital axis, and up, down, temporal, and nasal over about a 15° horizontal and vertical range. Each panel is an MRI scan plane, perpendicular to the orbital axis and 15 mm posterior to the globe-optic nerve junction.* ***A:*** *Even over this modest range of gaze, in the normal right eye, each muscle can be seen to contract (thicken) in its field of action. In particular, the right LR approximately doubles its cross-section during abduction, and the right SO approximately doubles its cross-section during depression. In contrast, the left LR and left SO show no contractility. Measurement shows that left MR contractility is also sub-normal. Comparing cross-sections in the two eyes, shows that the left LR is severely , and the LSO moderately atrophic.* ***B:*** *Following augmented vertical rectus transposition, little is changed in these posterior slices, although we note that the LSO has regained some contractility during the 6 weeks between scans.*

Eight weeks after chordoma surgery, strabismus surgery was performed, consisting of left superior rectus (SR) transposition to the superior end of the left LR insertion, with an augmentation suture on its inferior edge 8 mm posterior to the new insertion, and left IR transposition to the inferior end of the left LR insertion, with an augmentation suture on its superior edge 9 mm posterior. Postoperative alignment six weeks later shows excellent improvement in horizontal range, with little sacrifice of vertical range (figure 7-15A). MRI scans performed the same day are shown in figure 7-12B (3D reconstruction) and figure 7-14B.

Simulation of TS's strabismus surgery begins with the preoperative simulation of Figure 7-13B. We then simulate the left SRand left IR surgery done on TS (transposition is simulated by moving model insertions; a augmentation suture is estimated as a recess-resect, half the distance of the suture from the insertion). We suppose that the transposed muscles each stretch 5 mm, and that their pulleys stretch 7 mm medially, secondary to transposition. MRI scans show some recovery of right MR and LSO contractility (figure 7-14), on the basis of which we restore full left MR contractility, and set LSO contractility to 50% normal. Thus, we hypothesize that, whereas innervation to left LR was permanently lost, innervation to left MR was only temporarily impaired, and LSO innervation only partly impaired, by surgical trauma. The resulting simulation gives a reasonable match to TS's postoperative alignment measurements, except in extreme left gaze (figure 7-15B).

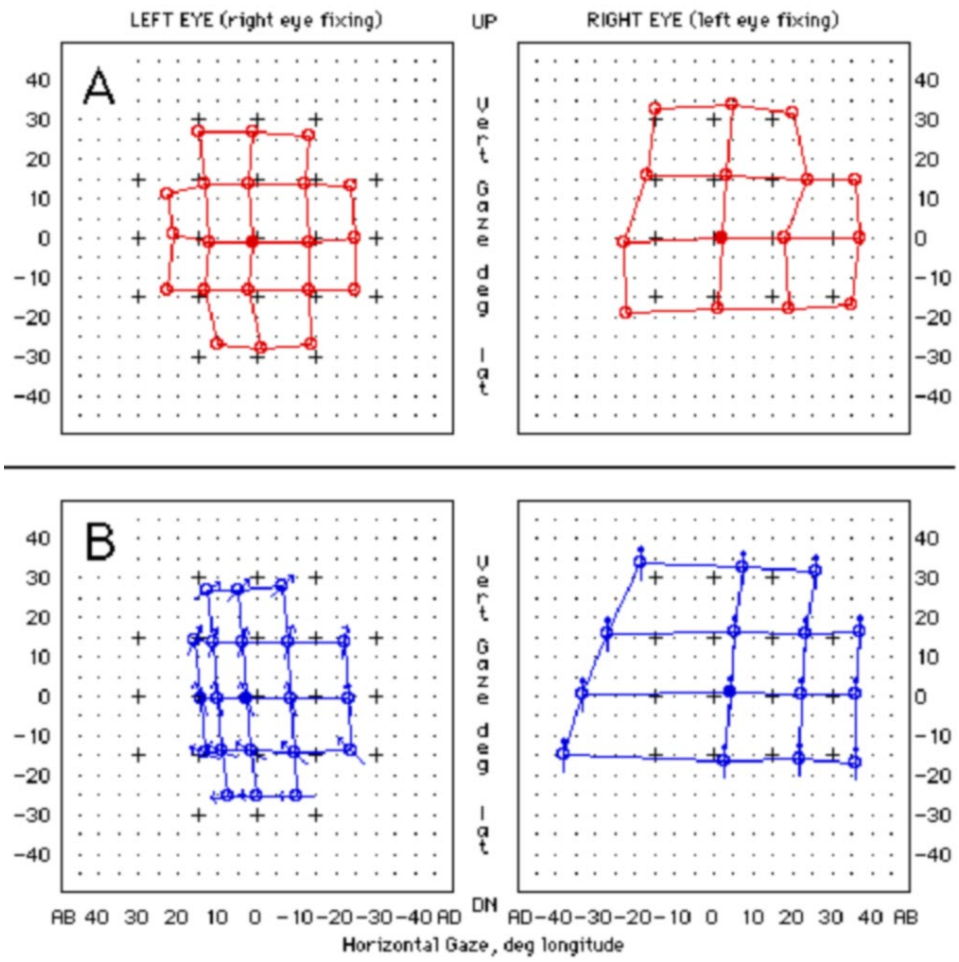

Figure 7-15. *Patient TS, binocular alignment after strabismus surgery.* ***A:*** *Clinical measurements. Left eye shows much improved horizontal range, with little sacrifice of vertical range. Right eye shows secondary deviations, much decreased compared to figure 7-13A.* ***B:*** *Simulation provides a good match to measurements, except in left gaze (see text).*

We cannot be sure why the simulation fails to match the clinical data in left gaze: there could be unsimulated orbital idiosyncrasies, errors in the clinical alignment data, or limitations in the biomechanical model. Perhaps TS's pre-existing horizontal diplopia is a clue, but we do not have enough information about it to form a hypothesis. Modeling can reduce, but not entirely eliminate clinical uncertainties.

Summary And Prospects

Predictions from computer models, confirmed by MRI in strabismus surgery patients, have shown the importance of the complex arrangements of connective tissues that support the extraocular muscles and determine their pulling directions. Immunohistochemistry then showed that mid-orbital connective tissues surrounding EOMs and coupling them to orbital walls contain smooth muscle cells, having sympathetic, parasympathetic and nitric

oxide mediated projections. Tracer and stimulation studies showed that the superior cervical ganglion was the source of the sympathetic projection. Thus, there is a substrate to support excitatory and inhibitory modulation of EOM pulling directions. Already, these findings have changed our understanding of extraocular muscle coordination providing, for instance, an orbital substrate for Listing's Law. Future research will determine if this system acts to refine eye alignment, aid vergence, or simply optimize the stiffness of these pulley-like connective tissue structures. As the clinical importance of extraocular connective tissues becomes clearer, it will be natural to study systemic connective tissue disorders, first as tests of emerging models, and then as cases in which new concepts can provide clinical guidance. Syndromes such as Marfan's and Williams', well characterized at a molecular level, are strongly associated with strabismus, and seem a natural place to begin studying the relationship of abnormal connective tissue to strabismus (Demer, et al, 1997 (submitted)).

More general biomechanical models must be developed to reflect mechanically important structures like the neurofibrovascular bundle (Stager, 1996; Stidham, et al, 1997), the lateral levator aponeurosis, and such strabismus surgeries as muscle splitting procedures.

Based on Robinson's (Robinson, 1975) model, the current Orbit model uses simplified, "string" muscles and tendons. Intrinsically 2-dimensional effects (e.g., the nonuniform distribution of force across the tendon's width due to tendon bending) are treated as special cases. Representations of muscle and tendon surfaces are only for appearance (e.g., muscles can intersect) (Miller, 1995). In a better model, tissue surfaces would be part of the biomechanical model, so that EOMs will deflect accurately when crossing (as when the SO emerges from the anterior edge of the SR). This will result in more accurate simulations (particularly of some surgeries) and more realistic graphic representations.

The scientific value of SQUINT and its successors lie in their ability to test and embody in a useful summary form, physiologic findings, clinical data, and theories of extraocular function. As imaging data become more used to characterize contractile and trophic states of EOMs (Miller, 1989; Demer, et al, 1994; Demer and Miller, 1995) and to describe structural abnormalities of orbits (Demer and Miller, 1997), it becomes more important to integrate imaging data into biomechanical modeling, thereby achieving better case simulations and better tests of the models.

Bibliography

Bicas, HEA (1972). Electo-oculography in the investigation of oculomotor imbalance - I. Basic aspects. *Vision Research,* vol 12, pgs 993-1010.

Burgerman, RS; **Wolf, AL**; **Kelman, SE**; **Elsner, H**; **Mirvis, S**; **Sestokas, AK (1989)**. Traumatic trochlear nerve palsy diagnosed by magnetic resonance imaging: Case report and review of the literature. *Neurosurgery,* vol 25, pgs 978-981.

Clark, RA; **Miller, JM**; **Demer, JL (1997a)**. Location and stability of rectus muscle pulleys inferred from muscle paths. *Invest Ophthalmol Vis Sci,* vol 38, pgs 227-240.

Clark, RA; Miller, JM; Rosenbaum, AL; Demer, JL (1997b). Heterotopic muscle pulleys or oblique muscle dysfunction? *Journal of Pediatric Ophthalmology and Strabismus*, vol In Press.

Clement, RA (1982). Computer simulation of extraocular muscle cooperation: An evaluation. *Ophthalmology and Physiological Optics*, vol 2, pgs 107-117.

Clement, RA (1985). A comparison of different models of extraocular muscle cooperation. *Ophthalmology and Physiological Optics*, vol 5, pgs 165-170.

Clement, RA; Howrie, A (1985). Computer modeling of the muscular factors involved in the etiology of A and V syndromes. *British Orthoptics Journal*, vol 42, pgs 65-68.

Demer, JL; Kerman, BM (1994). Comparison of standardized echography with magnetic resonance imaging to measure extraocular muscle size. *Am J Ophthalmol*, vol 118, isu 3, pgs 351-61.

Demer, JL; Miller, JM (1995). Magnetic resonance imaging of the functional anatomy of the superior oblique muscle. *Invest Ophthalmol Vis Sci*, vol 36, isu 5, pgs 906-13.

Demer, JL; Miller, JM (1997). Dynamic magnetic resonance imaging of the inferior oblique muscle in normal and strabismic subjects. *Abstracts of the Americal Association for Pediatric Ophthalmology and Strabismus*, vol In Press.

Demer, JL; Miller, JM; Koo, EY; Rosenbaum, AL (1994). Quantitative magnetic resonance morphometry of extraocular muscles: a new diagnostic tool in paralytic strabismus. *J Pediatr Ophthalmol Strabismus*, vol 31, isu 3, pgs 177-88.

Demer, JL; Miller, JM; Koo, EY; Rosenbaum, AL; Bateman, JB (ed). (1995a). *True versus masquerading superior oblique palsies: Muscle mechanisms revealed by magnetic resonance imaging*. cty Boca Raton (FL), pub CRC Press.

Demer, JL; Miller, JM; Poukens, V (1996). Surgical implications of the rectus extraocular muscle pulleys. *J Ped Ophthalmol Strabismus*, vol 33, isu 4 (July-Aug), pgs 208-218.

Demer, JL; Miller, JM; Poukens, V; Vinters, HV; Glasgow, BJ (1995b). Evidence for fibromuscular pulleys of the recti extraocular muscles. *Invest Ophthalmol Vis Sci*, vol 36, isu Invest Ophthalmol Vis Sci, pgs 1125-36.

Demer, JL; Miller, JM; Rosenbaum, AL (1992). Clinical correlations of models of orbital statics. In Scott, AB (Ed.), *Mechanics of Strabismus Symposium*, (pgs 141-161). San Francisco: Smith-Kettlewell Eye Research Institute.

Demer, JL; Poukens, V; A., CR; Miller, JM; Porter, JD (1997 (submitted)). Molecular mechanism of strabismus in Marfan syndrome (MFS): Deficient fibrillin destabilizes extraocular muscle pulleys. , vol *Ophthalmology* (supplement).

Demer, JL; Poukens, V; Micevych, P (1995c). Nitroxidergic and catecholaminergic innervation of the smooth muscle of the medial rectus pulley in humans. *Invest Ophthalmol Vis Sci*, vol 36, pgs S959.

Demer, JL; Poukens, V; Miller, JM; Micevych, P (1997). Innervation of extraoclar pulley smooth muscle in monkeys and humans. *Invest Ophthalmol Vis Sci*, vol 38, isu 9, pgs 1774-1785.

Feyerabend, P (1988). *Against Method.* edn rev. cty London, pub Verso.

Foster, RS (1997). Vertical muscle transposition augmented with lateral fixation. *Journal of AAPOS,* vol 1, isu 1, pgs 20-30.

Günther, S; Kusel, R; Rassow, B (1986). Midellmäßige Beschreibung der Augenmuskelwirkung unter Berücksichtigung des ligamentum Lockwood. *Fortschr Ophthalmol,* vol 83, pgs 514-517.

Guyton, DL; Weingarten, PE (1994). Sensory torsion as the cause of primary oblique muscle overaction/underaction in A- and V-pattern strabismus. *Binoc Vis Eye Muscle Surg Qtrly,* vol 9, pgs 209-236.

Hayes-Roth, F; Waterman, DA; Lenat, DB (1983). An overview of expert systems. In eds Hayes-Roth, F, Waterman, DA and Lenat, DB, *Building Expert Systems* , . cty Reading, MA, pub Addison-Wesley.

Howrie, A; Clement, RA (1986). Computer modeling of anomalous innervation of the extra-ocular muscles. *British Orthoptics Journal,* vol 43, pgs 56-60.

Konen, W; Rüssman, W (1982). Kleinrechnerprogramme zur strabologischen operationsindikation. *Fortschr Ophthalmol,* vol 79, pgs 550-551.

Kuhn, TS (1970). *The Structure of Scientific Revolutions.* edn 2. cty Chicago, pub University of Chicago Press.

Kusel, R; Haase, W (1977). Versuch einer mathematischen Darstellung der Augenmuskelwirkung. *Ber Dtsch Ophthalmol,* vol 45, pgs 453-458.

Miller, JM (1984). Computer model of binocular alignment. In Semmlow, JL and Welkowitz, W (Ed.), *Sixth Annual Conference, IEEE Engineering in Medicine and Biology Society*, . New York, NY:

Miller, JM (1985). Applications of the SQUINT computer strabismus model. In *Association for Research in Vision and Ophthalmology,* 26 (pgs 253). Sarasota, FL: Investigative Opthalmology and Visual Science.

Miller, JM (1989). Functional anatomy of normal human rectus muscles. *Vision Res,* vol 29, isu 2, pgs 223-40.

Miller, JM (1995). *Orbit™ 1.5 Gaze Mechanics Simulation User's Manual* No. Eidactics; Suite 404; 1450 Greenwich Street; San Francisco, CA 94109; USA.

Miller, JM; Demer, JL (1992). Biomechanical analysis of strabismus. *Binocular Vision and Eye Muscle Surgery Quarterly,* vol 7, isu 4, pgs 233-248.

Miller, JM; Demer, JL; Rosenbaum, AL (1993). Effect of transposition surgery on rectus muscle paths by magnetic resonance imaging. *Ophthalmology,* vol 100, isu 4, pgs 475-87.

Miller, JM; Robinson, DA (1984). A model of the mechanics of binocular alignment. *Comput Biomed Res,* vol 17, isu 5, pgs 436-70.

Miller, JM; Shamaeva, I; Pavlowski, DS (1996). *Orbit™ 1.6 Gaze Mechanics Simulation.* cty San Francisco, pub Eidactics.

Neetens, A; Janssens, M (1979). The superior oblique: A challenging extraocular muscle. *Doc Ophthalmol*, vol 46, pgs 295-303.

Park, C; Miller, JM; Demer, JL (1996). Computational simulation of concomitant horizontal strabismus. *Invest Ophthalmol Vis Sci ARVO Abstract*, vol 37, pgs S490.

Parks, MM; Wheeler, MB (1996). Concomitant Esodeviations. In eds Tasman, W and Jaeger, EA, *Clinical Ophthalmology* , . cty Philadelphia, pub Lippincott-Raven.

Partridge, LD; Benton, LA (1982). Muscle, the motor. In eds *Handbook of Physiology -- the Nervous System II.* , . cty Baltimore, pub American Physiological Society.

Porter, JD; Poukens, V; Baker, RS; Demer, JL (1995). Cytoarchitectural organization of the medial rectus muscle pulley in man. *Invest Ophthalmol Vis Sci*, vol 36, pgs S960.

Porter, JD; Poukens, V; Baker, RS; Demer, JL (1996). Structure-function correlations in the human medial rectus extraocular muscle pulleys. *Invest Ophthalmol Vis Sci*, vol 37, isu 2, pgs 468-72.

Robinson, DA (1975). A quantitative analysis of extraocular muscle cooperation and squint. *Invest Ophthalmol*, vol 14, isu 11, pgs 801-25.

Ruete, CGT (1857). *Ein neues Ophthalmotrop, zur Erläuterung der Functionen der Muskeln und brechenden Medien des menschlichen Auges*. cty Leipzig, pub Teubner.

Rüssman, W (1982). Microcomputer use in planning strabismus surgery. In *Proceedings of Meeting of International Strabismological Association*, (pgs 299-302). Florence:

Scott, AB (1994). Change of eye muscle sarcomeres according to eye position. *J Pediatr Ophthalmol Strabismus*, vol 31, isu 2, pgs 85-8.

Scott, AB; Miller, JM; Collins, CC (1992). Eye muscle prosthesis. *J Pediatr Ophthalmol Strabismus*, vol 29, isu 4, pgs 216-8.

Simonsz, HJ (1990). A pocket-computer program for oblique muscle surgery. *J Pediatr Ophthalmol Strabismus*, vol 27, isu 2, pgs 84-7.

Simonsz, HJ; Spekreijse, H (1996). Robinson's computerized strabismus model comes of age. *Strabismus*, vol 4, isu 1, pgs 25-40.

Stager, DR (1996). The neurofibrovascular bundle of the inferior oblique muscle as its ancillary origin. *Trans Am Ohthalmol Soc*, vol 94, pgs 1073-1094.

Stidham, DB; Stager, DR; Kamm, KE; Grange, RW (1997). Stiffness of the inferior oblique neurofibrovascular bundle. *Invest Ophthalmol Vis Sci*, vol 38, pgs 1314-1320.

Williams, PE; Goldspink, G (1978). Changes in sarcomere length and physiological properties in immobilized muscle. *Journal of Anatomy*, vol 127, pgs 459-468.

Wundt, W (1862). Über die Bewegung der Augen. *Archive für Ophthalmologie*, vol 8, isu 2, pgs 1-87.